IEEE Computer Society Workshop on
Mathematical Methods in Biomedical
Image Analysis (MMBIA 2006)

Interpolation in Discrete Single Figure Medial Objects

Qiong Han, Stephen M. Pizer, James N. Damon
Medical Image Display & Analysis Group (MIDAG)
University of North Carolina at Chapel Hill
han@cs.unc.edu

Abstract

The discrete m-rep, a medial representation of anatomical objects made from one or more meshes of medial atoms, has many attractive properties for biomedical image analysis. The nonlinear nature of the m-rep parameters captures nonlinear deformations in anatomical objects such as twisting and bending. Most uses of m-reps require extending them to one or more continuous sheets of medial atoms. To guarantee that a continuous sheet of medial atoms does not fold, we propose an interpolation method on the medial atoms based on two medial shape operators. *The* radial shape operator *describes the rate of swing of a medial atom's spoke. The* edge shape operator *describes the rate of swing of a planar curve defining the object crest. The two shape operators generate interpolated internal and end atoms, and they join together smoothly. We show the application of our interpolation method on m-reps of synthetic and real-world objects.*

1. Introduction

Medial representations of anatomical objects represent both the surface boundaries and the interior of those objects. The m-rep as one of the 2D and 3D medial representations has been used in medical image segmentation and shape analysis. It leads to effective probability distribution of the non-linear object shape variations [1] and of the image intensity appearance associated to the object-relative image regions [2]. Using such trained probability distributions as the priors, segmentation based on the posterior optimization (MAP) has been shown to be effective [2].

The effectiveness of the m-rep results from its nonlinear representation of both the surface and the interior of an anatomical object. Recent work indicates that the m-rep sometimes better captures the deformations of anatomical objects such as bending and twisting than boundary representations such as the point distribution model.

There are generally two forms of m-reps: cm-reps [3, 4] and discrete m-reps [5, 6]. A cm-rep represents an anatomical object with a continuous and parameterized *medial axis* while a discrete m-rep represents the object by a set of samples or adapted samples from the continuous medial locus of so-called *medial atoms*.

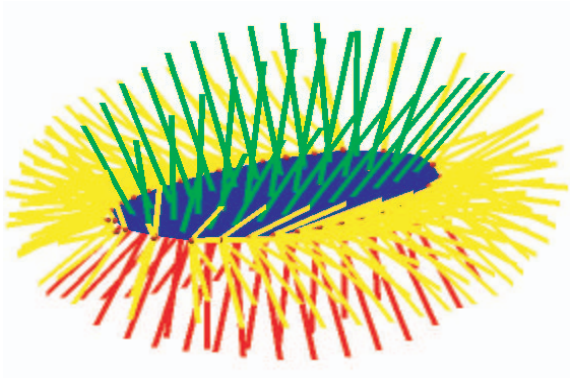

Figure 1. Demonstration of the interpolated spoke fields from a discrete m-rep: the medial sheet (in dark blue) with an end curve as its boundary, the interpolated spokes (red and green on each side of the medial sheet) for the internal region, and the interpolated spokes (yellow) for the crest region.

A cm-rep is composed of a smooth medial sheet and a radius field defined on the sheet. It provides a continuous and parameterized representation of the object volume. The entire volume defined within the object surface is parameterized via the smooth spoke field derived from a radius r field on the *medial sheet* surface $\mathbf{x}(u, v)$, shown as the dark blue surface in fig. 1. The volume parameterization of an anatomical object provides a coordinate system for the 3D volume so that the 3D image of the object can be uniquely parameterized and accessed. In addition, we can use medial atom information to model inter-object relations within a complex of objects. Also, reparameterizations used to produce good correspondence across anatomical objects, a requirement for statistical analysis on the geometry of objects, needs a continuous locus.

A discrete m-rep is composed of a set of medial atoms. Although it does not automatically give a continuous representation of the object, the discrete m-rep provides local-

ized control over the object shape that the cm-rep does not provide. If we can interpolate the set of medial atoms by deriving a continuous medial representation of the object from its discrete m-rep, we can benefit from having a continuous medial representation and still capture the more localized shape variations by the medial atoms.

The interpolation of points in $\mathbb{R}^3$ has been well studied. In our case each discrete medial atom lies in a curved Riemannian space and the methods in $\mathbb{R}^3$ do not directly apply. This paper proposes a method of interpolating discrete m-reps based on the differential geometric properties of the medial axis, the combination of the medial sheet and the spoke fields on it.

From differential geometry of 3D surface, the *shape operator* of a 3D surface tells us the properties such as Gaussian curvatures of the 3D surface. That shape operator contains the information of how the surface normal at a surface point changes while walking in the tangent plane at that surface point. James Damon's recent work [7, 8, 9] applies the differential geometry method to the medial axis, and he defined the *radial shape operator* and *edge shape operator* for the interior and the end crest curve of a medial axis, respectively. The shape operators of a medial spoke field are analogous to the regular shape operator of a 3D surface: the radial shape operator tells how a spoke changes while walking on the medial sheet surface and the edge shape operator tells the rate of spoke change along the end curve of the medial sheet. Damon also showed a set of conditions to maintain the legality of the implied surface boundary by the continuous spoke field, which enables us to work directly on the continuous spoke field attached to the medial sheet. The spoke field with a legal surface boundary ensures a unique parameterization of both the surface and the interior of the object. Both the radial/edge shape operators and the legality conditions will be used in our interpolation.

It has also been shown that the discrete m-rep can represent objects with multiple parts [10, 11]. The ability of interpolating between the parts of such objects is of great interest as well. However in this paper we focus on the interpolation in a single medial atom mesh. The goal is to derive a continuous representation for any single figure objects provided in discrete form.

The rest of this paper is organized as the follows. The next section reviews some of the previous attempts on m-rep interpolation. Section 3 details the interpolation method on single figure m-reps. Section 4 shows the results, discusses some open issues and future work, and concludes this paper.

2. Previous Work on M-Rep Interpolation

For discrete boundary based representations, the interpolation is typically on the boundary points. The essential difference between the interpolation of the boundary points and a medial structure of the object is that the former does not incorporate the normal information into the interpolation. There could be improper shapes from the interpolation such as surface ripples or even creases due to the lack of any explicit control on the surface normals.

In computer graphics work has been done on boundary point interpolation with the consideration of the surface normals. Thall tried to incorporate the normal information into the Catmull-Clark subdivision based interpolation of the boundary implied by a discrete m-rep [12]. He post-processed the interpolated surface boundary from the subdivision by rotating the local patch around each surface control point to match the surface normal at that point to the one implied by the medial atoms. Due to the locality of the post-processing, Thall's method may generate unexpected ripples. Moreover, interpolation on both boundary points and normals still does not guarantee a valid parameterization of the volume within the object boundary. If we march along the normals into the interior of the object, we do not know how far to go before the normal profiles across one another.

The interpolation on the medial representation however gives both valid surface points and the associated surface normals automatically. There is an available method to interpolate the medial atoms that uses the existing interpolation methods in $\mathbb{R}^3$ to calculate the interpolation weights, which are then used in the weighted geodesic average on the control atoms to get the interpolated medial atom.

Given N atom $\{\mathbf{A}_i = (\mathbf{p}_i, r_i, \mathbf{u}_i^+, \mathbf{u}_i^-) \in \mathbf{M} = \mathbb{R}^3 \times \mathbb{R}^+ \times \mathcal{S}^2 \times \mathcal{S}^2, i = 1, 2, ..., N\}$ and the weight list $\omega = (\omega_1, \omega_2, ..., \omega_N)$, the interpolated atom $\mathbf{A}(\omega)$ is defined as

$$\mathbf{A}(\omega) = \arg\min_{\mathbf{A}} \sum_{i=1}^{N} \omega_i \cdot dis^2(\mathbf{A}, \mathbf{A}_i) \qquad (1)$$

Each $\mathbf{A}_i$ lies on a Riemannian manifold, so the weighted average is based on the geodesic distance $dis(\mathbf{A}, \mathbf{A}_i)$ between the two atoms $\mathbf{A}$ and $\mathbf{A}_i$ in $\mathbf{M}$. When the weights ω are all equal, e.g. $\{\omega_i = \frac{1}{N}, \text{ for all } i\}$, the interpolated atom is exactly the Fréchet (intrinsic) mean of the N atoms $\mathbf{A}_i$. If $N = 2$ and $\omega = (1 - \omega_2, \omega_2)$, $\mathbf{S}(\omega_2)$ $(\omega_2 \in [0, 1])$ forms the exact geodesic path between $\mathbf{A}_0$ and $\mathbf{A}_1$. For arbitrary N and ω, (1) defines $\mathbf{A}(\omega)$ as the general weighted geodesic average of the N atoms.

(1) is a minimization problem. The existence and uniqueness of the solution to the problem are not generally ensured. However, it has been discussed in [1] that the solution to the minimization problem exists and is unique if the data are well-localized. In the case of m-reps the interpolation is done among neighboring atoms, which are not too far away from one another. The interpolation based on (1) is expected to converge well and yield unique solutions. Empirically the interpolated atom $\mathbf{A}(\omega)$ has been successfully calculated for different control atoms $\{\mathbf{A}_i\}$ and weights ω.

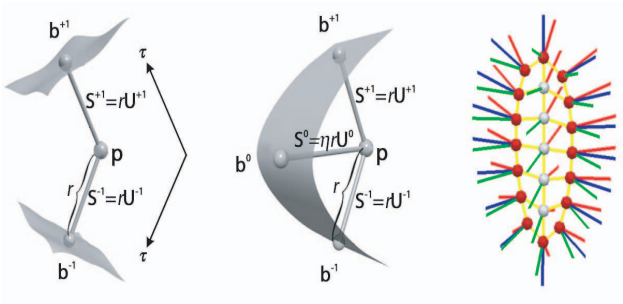

Figure 2. Left: an internal atom of two spokes $\mathbf{S}^{+1}$ and $\mathbf{S}^{-1}$, with τ to parameterize the object interior along the spokes. Middle: an end atom with an extra bisector spoke $\mathbf{S}^0$. Right: a discrete m-rep as a mesh of internal atoms (with white hubs) and end atoms (with red hubs).

The minimization in (1) ends up optimizing each one of the atom components separately. The interpolation using geodesic average of the medial atoms might still yield improper surfaces because it inadequately reflects the relations within all the components of a medial atom: the atom hub position, atom spoke length, and atom spoke direction.

In next section we propose a medial atom interpolation based on the radial shape operator, which represents how a medial atom changes on the medial sheet. In other words the radial shape operator plays an explicit role in the interpolation and reflects the related changes in all the components of the medial atom.

3. Atom Interpolation in Discrete Medial Objects

A continuous medial locus has interior points and end points, with the latter corresponding to the crest region of the boundary. Correspondingly, each discrete m-rep of a single figure anatomical object is composed of two types of medial atoms: internal and end atoms. We will start this section by reviewing the definitions of the two types of medial atoms. We then address the details of both internal and end atom interpolation followed by the generation of the crest region.

3.1. Medial Atoms in Discrete M-Reps

As shown in fig. 2, an internal medial atom $\mathbf{A}$ is given as $\{\mathbf{p}, r, \mathbf{U}^{+1}, \mathbf{U}^{-1}\}$. The two spokes of each internal atom are $\mathbf{S}^{+1/-1} = r\mathbf{U}^{+1/-1}$, where $\mathbf{U}^{+1/-1}$ are unit vectors for spoke directions. An end atom has one extra parameter η determining the length of a bisector spoke as $\mathbf{S}^0 = r\eta\mathbf{U}^0$, where $\mathbf{U}^0 = \frac{\mathbf{U}^{+1}+\mathbf{U}^{-1}}{\|\mathbf{U}^{+1}+\mathbf{U}^{-1}\|}$. The end atom in a discrete m-rep is not the same as the end atom in the Blum case [13]. In the strict Blum case, when we approach the end of the medial sheet from an internal point, the two spokes of the sampled atoms swing close to each other and finally collapse into one single spoke at the very end of the medial sheet. In order to have more stability in the representation, a discrete m-rep has the hub $\mathbf{p}$ of each end atom not lying on the exact end of the medial sheet. Instead the end of the medial sheet is $\mathbf{p}+r(\eta-1)\mathbf{U}^0$, which is on the bisector spoke of an end atom.

Each end atom can be considered as the compound of an internal atom $\{\mathbf{p}, r, \mathbf{U}^{+1}, \mathbf{U}^{-1}\}$ plus the bisector spoke corresponding to the crest line on the object boundary. The hub position and two regular spokes $\mathbf{S}^{+1/-1}$ of each end atom are treated as one of the internal atom and will be interpolated with other internal atoms. The results from that interpolation give the hub positions and the two regular spokes as the basis for the end atom interpolation. The extra bisector spokes $\mathbf{S}^0$ of an end atom lie in the same plane with $\mathbf{S}^{+1/-1}$. They form a planar cross section in the object crest region. That planarity will be used in the further interpolation of end atoms.

The two types of atoms represent different parts of a medial axis, each with different interpolation. The following two subsections cover the details of the interpolations of the internal and end atoms, respectively.

3.2. Interpolation of Internal Medial Atoms

Each internal medial atom $\{\mathbf{p}, r, \mathbf{U}^{+1}, \mathbf{U}^{-1}\}$ has the hub position $\mathbf{p}$ as the linear part and the pair of spokes $\{\mathbf{S}^{+1/-1} = r\mathbf{U}^{+1/-1}\}$ as the nonlinear part. We first interpolate the hub positions $\mathbf{p}$ of internal atoms using the point and normal interpolation to form a continuous medial sheet $\mathbf{x}(v_1, v_2)$. Then we interpolate the radial shape operators for the interpolation legality. Finally the interpolated medial sheet and radial shape operators are used in the spoke interpolation by integration to get the full interpolated atom.

3.2.1 Medial sheet $\mathbf{x}(v_1, v_2)$ interpolation

The hub position $\mathbf{p}$ forming the medial sheet $\mathbf{x}(v_1, v_2)$ is a point in $\mathbb{R}^3$. At each control atom, the normal to the medial sheet $\mathbf{x}(v_1, v_2)$ is also given by the difference of the two spokes $\frac{\mathbf{U}^{+1}-\mathbf{U}^{-1}}{\|\mathbf{U}^{+1}-\mathbf{U}^{-1}\|}$. With the points and normals both known at all the control points, the medial sheet $\mathbf{x}$ is interpolated by a point and normal interpolation based on the cubic Hermite patch interpolation.

The cubic Hermite patch is chosen because it allows specifying the tangent directions of the medial sheet at the control points. By enforcing the tangent directions at the control points to be perpendicular to the given normals, we can have a continuous and parameterized medial sheet $\mathbf{x}(v_1, v_2)$ that interpolates both points and normals given by the control atoms. The cubic Hermite patch also leaves four extra free parameters for more potential constraints.

The medial sheet interpolation is in a local quad patch of four control atoms, using the four hub positions and eight

tangent directions (two from each atom) implied by the four control atoms. C^1 continuity is achieved across the patch boundaries. Since the cubic Hermite patch has an explicit form, the derivatives $\mathbf{x_u}$ of the medial sheet surface $\mathbf{x}(\mathbf{u})$ are analytically evaluated and will be used in the spoke interpolation.

3.2.2 Spoke $\mathbf{S}(v_1, v_2)$ interpolation

The nonlinear part of each internal atom $\{\mathbf{p}, r, \mathbf{U}^{+1}, \mathbf{U}^{-1}\}$ is the pair of spokes $\{\mathbf{S}^{+1/-1} = r\mathbf{U}^{+1/-1}\}$. The two spokes of each internal atom form a double valued spoke field on the medial sheet surface. As briefly described in section 1, a term called the radial shape operator defined by James Damon is analogous to the regular shape operator of a 3D surface. The radial shape operator contains the information of how the spokes changes while we walk on the medial sheet surface, and it also determines a set of legality conditions for the m-rep implied boundary. The radial shape operator will be needed to interpolate the atom spokes, so it is important to better understand the radial shape operator. The background of the radial shape operator will be reviewed next. It provides a means for maintaining the legality of the interpolated spoke field and nicely combines together all the atom components.

3.2.3 Overview of the radial shape operator

Damon applied the differential geometry on the Blum's medial axis and extended the regular shape operator to the medial case. Analogously, the radial shape operator tells how a medial spoke changes while walking on the medial sheet. The incorporation of the legality conditions into the discrete m-rep framework allows the direct control on the legality of the implied boundary. Recall that each internal m-rep atom has two spokes at both sides of the medial sheet, the spoke fields on the medial sheet should be considered as double valued. So there are two radial shape operators defined for each atom: one for each spoke at one side of the medial sheet.

Let us only consider one side of the medial sheet since the same method applies to the other side. Assume that there is a continuous spoke field $\mathbf{S}(\mathbf{u})$ with unit length spoke direction $\mathbf{U}(\mathbf{u})$ and spoke length $r(\mathbf{u})$ on one side of the continuous medial sheet $\mathbf{x}(\mathbf{u})$ as $\mathbf{S}(\mathbf{u}) = r(\mathbf{u}) \cdot \mathbf{U}(\mathbf{u})$, and $\mathbf{u} = (v_1, v_2)$ parameterizes the two dimensional medial sheet and the spoke field on one side of sheet. The derivatives of the unit length spoke direction $\mathbf{U}(\mathbf{u})$ by (v_1, v_2) are calculated as follows, with $\mathbf{U}, \mathbf{x}_{v_1/v_2}$ being 1×3 row vectors.

$$\frac{\partial \mathbf{U}}{\partial v_i} = a_{0,i}\mathbf{U} - a_{i,1}\mathbf{x}_{v_1} - a_{i,2}\mathbf{x}_{v_2}, \text{ where } i = 1, 2, \quad (2)$$

or rewriting in matrix form:

$$\frac{\partial \mathbf{U}}{\partial \mathbf{u}} = \begin{pmatrix} a_{0,1} \\ a_{0,2} \end{pmatrix} \mathbf{U} - \begin{pmatrix} a_{1,1} & a_{1,2} \\ a_{2,1} & a_{2,2} \end{pmatrix} \begin{pmatrix} \mathbf{x}_{v_1} \\ \mathbf{x}_{v_2} \end{pmatrix} \quad (3)$$

where $\frac{\partial \mathbf{U}}{\partial \mathbf{u}}$ is a 2×3 matrix with row i as the vector $\frac{\partial \mathbf{U}}{\partial v_i}$; $\mathbf{x}_{v_1}$ and $\mathbf{x}_{v_2}$ are the derivatives of the medial sheet $\mathbf{x}$ by parameters v_1 and v_2. In these equations, the derivative of $\mathbf{U}$ is decomposed by a generally non-orthogonal projection along the spoke direction $\mathbf{U}$ to the tangent plane of the medial sheet spanned by $\mathbf{x}_{v_1}$ and $\mathbf{x}_{v_2}$.

Let $\mathbf{A_u} = \begin{pmatrix} a_{0,1} \\ a_{0,2} \end{pmatrix}$, and $\mathbf{S}_{rad} = \begin{pmatrix} a_{1,1} & a_{2,1} \\ a_{1,2} & a_{2,2} \end{pmatrix}$. $\mathbf{S}_{rad}$ is called the radial shape operator. In general, the radial shape operator is a 2×2 matrix that is not self-adjoint.

Then (3)⇒

$$\frac{\partial \mathbf{U}}{\partial \mathbf{u}} = \mathbf{A_u}\mathbf{U} - \mathbf{S}_{rad}^T \begin{pmatrix} \mathbf{x}_{v_1} \\ \mathbf{x}_{v_2} \end{pmatrix} \quad (4)$$

$\mathbf{U}(\mathbf{u})$ is of unit length, $\frac{\partial \mathbf{U}}{\partial \mathbf{u}} \cdot \mathbf{U}^T = \begin{pmatrix} 0 \\ 0 \end{pmatrix}$ and $\mathbf{U} \cdot \mathbf{U}^T = 1$, so

$$\mathbf{A_u} = \mathbf{S}_{rad}^T \begin{pmatrix} \mathbf{x}_{v_1} \\ \mathbf{x}_{v_2} \end{pmatrix} \mathbf{U}^T \quad (5)$$

Substituting (5) into (4) yields the means of computing $\mathbf{S}_{rad}$ given $\frac{\partial \mathbf{U}}{\partial \mathbf{u}}$, $\mathbf{U}$ and $\begin{pmatrix} \mathbf{x}_{v_1} \\ \mathbf{x}_{v_2} \end{pmatrix}$. That is, $\mathbf{S}_{rad}$ depends on the spoke direction $\mathbf{U}$, and the derivatives of $\mathbf{U}$ and $\mathbf{x}$.

However, $\mathbf{S} = r\mathbf{U}$ is what we aim to interpolate. The derivative of a full spoke $\mathbf{S} = r\mathbf{U}$ with length r is given as follows.

$$\frac{\partial \mathbf{S}}{\partial \mathbf{u}} = \frac{\partial (r\mathbf{U})}{\partial \mathbf{u}} = r\frac{\partial \mathbf{U}}{\partial \mathbf{u}} + \begin{pmatrix} r_{v_1} \\ r_{v_2} \end{pmatrix} \mathbf{U} \quad (6)$$

Substituting (4) and (5) into (6) yields

$$\frac{\partial \mathbf{S}}{\partial \mathbf{u}} = r\mathbf{S}_{rad}^T \begin{pmatrix} \mathbf{x}_{v_1} \\ \mathbf{x}_{v_2} \end{pmatrix} (\mathbf{U}^T\mathbf{U} - \mathbf{I}) + \begin{pmatrix} r_{v_1} \\ r_{v_2} \end{pmatrix} \mathbf{U} \quad (7)$$

From Damon, a compatibility condition requires that $r_{v_1/v_2} = -\mathbf{x}_{v_1/v_2}\mathbf{U}^T$. Let $Q = \begin{pmatrix} \mathbf{x}_{v_1} \\ \mathbf{x}_{v_2} \end{pmatrix} (\mathbf{U}^T\mathbf{U} - \mathbf{I})$ as a 2×3 matrix. Then

$$r\mathbf{S}_{rad} = \left(\left(\frac{\partial \mathbf{S}}{\partial \mathbf{u}} + \begin{pmatrix} \mathbf{x}_{v_1}\mathbf{U}^T \\ \mathbf{x}_{v_2}\mathbf{U}^T \end{pmatrix} \mathbf{U} \right) \mathbf{Q}^T (\mathbf{Q}\mathbf{Q}^T)^{-1} \right)^T \quad (8)$$

(8) shows how to compute $r\mathbf{S}_{rad}$ given the derivative of $\mathbf{S}$, $\mathbf{x}$ and $\mathbf{U}$. Conversely if we know $r\mathbf{S}_{rad}$ at each point on the medial sheet, we can calculate the derivative of $\mathbf{S}$ and recover the full spoke field $\mathbf{S}(\mathbf{u})$, given the known boundary conditions. This applies for the spokes on both sides of the medial sheet.

Analogously with the meaning of the eigenvalues and eigenvectors of the shape operator for a surface point in $\mathbb{R}^3$, Damon named the eigenvalues of the radial shape operator $\mathbf{S}_{rad}$ the *principal radial curvatures* κ_{ri}, and he named the eigenvectors the *principal radial directions*. He showed that for a legal spoke field, i.e., one free of any intersections among the spokes, $\kappa_{ri} < 1$ for all positive principal radial curvatures $\kappa_{ri,i=1,2}$ of $r\mathbf{S}_{rad}$.

With this radial curvature condition we can ensure the smoothness of the implied boundary for all the internal atoms. Moreover $r\mathbf{S}_{rad}$ for the full spokes $\mathbf{S}$ represent the combined rate of change of both the medial sheet $\mathbf{x}$ and full spokes $\mathbf{S}$. Basing the internal atom interpolation on the radial shape operator becomes a natural choice. However this requires $r\mathbf{S}_{rad}$ to be interpolated as well. We describe this interpolation next.

3.2.4 $r\mathbf{S}_{rad}$ interpolation

The radial shape operators at control atoms are first numerically estimated, assuring that they meet the radial curvature legality condition. By interpolating their eigenvalues and eigenvectors, we can assure the interpolands' legality, as follows.

We interpolate the two eigenvalues $\kappa_{i,1/2}$ by treating each $(1 - \kappa_{i,1/2})$ as an element in the multiplicative Lie group $\mathbb{R}^+$. The eigenvectors are considered as the elements in $\mathcal{SO}(2)$ and interpolated in the same group. The interpolation in $\mathcal{SO}(2)$ can be analytically calculated without any optimization. The interpolated eigenvalues and eigenvectors are then combined into a legal radial shape operator by the inverse eigen-decomposition.

One potential problem with the $r\mathbf{S}_{rad}$ interpolation is the existence of medial umbilic points, where the radial shape operator does not have a real eigen-decomposition to calculate the eigenvalues and eigenvectors. In section 4.2 we will discuss the possible solution for this. Next, we will go into the details of the internal atom interpolation.

3.2.5 Internal atom interpolation by integration

Given the interpolated medial sheet and $r\mathbf{S}_{rad}$, we can compute $\frac{\partial \mathbf{S}}{\partial \mathbf{u}}$ as described earlier and integrate it to produce the spokes. These spoke functions are guaranteed to be legal. The algorithm for internal atom interpolation is applied not only to the regions surrounded by internal spokes but also to regions bounded by the end atoms using their regular spokes. It consists of the following steps.

1. We interpolate the medial sheet $\mathbf{x}(v_1, v_2)$ by points and normals given by control atoms;
2. $\{r\mathbf{S}^{+1/-1}_{rad,i,i=0,\ldots,N}\}$ are calculated for the given control atoms (for both sides of the medial sheet);
3. The radial shape operators are interpolated as $r\mathbf{S}^{+1/-1}_{rad}(v_1, v_2)$;
4. Given the interpolated medial sheet and radial shape operators, the first-order derivative $\frac{\partial \mathbf{S}^{+1/-1}}{\partial \mathbf{u}}$ of the spokes $\mathbf{S}$ is calculated by (5) and (7);
5. The spoke $\mathbf{S}^{+1/-1}(v_1, v_2)$ is interpolated by an integration:

$$\mathbf{S}^{+1/-1}_{(v_1,v_2)} = \mathbf{S}^{+1/-1}_{(0,0)} + \int_{0:(0,0)}^{1:(v_1,v_2)} \left(\frac{\partial \mathbf{S}^{+1/-1}}{\partial u} du + \frac{\partial \mathbf{S}^{+1/-1}}{\partial v} dv\right) \tag{9}$$

6. $\mathbf{S}^{+1/-1}(v_1, v_2)$ gives both $\mathbf{U}^{+1/-1}(v_1, v_2) = \frac{\mathbf{S}^{+1/-1}(v_1,v_2)}{\|\mathbf{S}^{+1/-1}(v_1,v_2)\|}$ and $r(v_1, v_2) = \|\mathbf{S}^{+1/-1}(v_1, v_2)\|$;
7. The interpolated atom is $\mathbf{A}(v_1, v_2) = (\mathbf{x}(v_1, v_2), r(v_1, v_2), \mathbf{U}^{+1}(v_1, v_2), \mathbf{U}^{-1}(v_1, v_2))$;

$\frac{\partial \mathbf{S}^{+1/-1}}{\partial v_1}$ and $\frac{\partial \mathbf{S}^{+1/-1}}{\partial v_2}$ are calculated by (5) and (7) from the interpolated $r\mathbf{S}^{+1/-1}_{rad}(v_1, v_2)$.

The next section describes the interpolation of end atoms and the generation of the crest region, by extending the ideas of using the radial shape operator to Damon's edge shape operator.

3.3. Interpolation of End Medial Atoms and Generation of the Crest

Interpolation of the end atoms is based on the results from internal atom interpolation. The continuous hub positions $\mathbf{p}$ forming the end curve of the medial sheet and two regular spokes $\mathbf{S}^{+1/-1}$ of each interpolated end atom $(\mathbf{p}, \mathbf{S}^{+1/-1} = r\mathbf{U}^{+1/-1}, \eta)$ are given by the internal atom interpolation. Also, the bisector spoke direction at each interpolated atom is implied as $\mathbf{U}^0 = \frac{\mathbf{U}^{+1}+\mathbf{U}^{-1}}{\|\mathbf{U}^{+1}+\mathbf{U}^{-1}\|}$. The free parameter η is interpolated by a cubic Hermite interpolation from the η's of end control atoms. What's left to be done is as follows.

For each interpolate end atom with three spokes, generate a series spokes smoothly filling the gaps between $\mathbf{S}^{+1}, \mathbf{S}^0$ and $\mathbf{S}^0, \mathbf{S}^{-1}$. Since all three spokes of each end atom are coplanar, the filling spokes are all planar, and their spoke ends form a planar curve. This interpolation must be done in a way ensuring that the series of the planar curves sweeping along the end curve of the medial sheet yield a legal crest region. We accomplish these goals as follows.

1. A part of an ellipse is fit to interpolate the three spoke ends of each end atom, while keeping the orthogonality between the ellipse curve and the spokes at the spoke ends. By this means the curve is connected smoothly to the implied boundary by the interpolated internal atom, and the medial sheet of the partial ellipse lies on the bisector spoke as a segment.

2. All the planar curves for interpolated end atoms form a sweeping surface along the medial sheet end curve,

and that generates the crest region. A legality condition for crest from Damon is then used to detect any illegality, which would be removed by changing the η interpolation. The end curve of the medial sheet from the internal atom interpolation provides the edge coordinates that are needed.

Different from the internal atom interpolation, the legality of the interpolated end atoms is not maintained directly during the interpolation because it depends on how the three spokes from each end atom are interpolated. However the legality of the implied crest boundary is checked by a simple condition derived from the crest generation method. Any illegality detected in the crest requires changing the η interpolation for end atom bisector spokes.

The legality condition for the crest region is derived by Damon based on his edge shape operator. In the rest of this section, we will review the edge shape operator first, describe how each planar curve is created from the three spokes of each interpolated end atom, show the adapted and simple legality condition for the crest region generated by sweeping planar curves, and summarize the end atom interpolation.

3.3.1 Overview of the edge shape operator $r\mathbf{S}_E$

In contrast to internal atoms, the hub positions of end atoms lie on the end curve of the medial sheet, which requires a one-dimensional coordinate system. The medial sheet interpolation in section 3.2.1 provides the end curve $\delta(t)$ of the medial sheet. $\delta(t)$ is C^1 continuous except for the four "corners" and provides the edge coordinates for the end atoms. Given that, assume $\mathbf{x}(w_1, w_2)$ is a local edge parameterization of an open set W with $\mathbf{x}(0,0) = \mathbf{x}_0$ as one point on end curve such that for $\mathbf{y}_i = \frac{\partial \mathbf{x}}{\partial w_i}, i = 1, 2, \mathbf{y}_1 \in \boldsymbol{T}_{\mathbf{x}_0}\delta(t)$ as the tangent of the end curve $\delta(t)$ and $\mathbf{y}_2$ maps under the edge parameterization to $c\mathbf{U}_{tan}$, for $\mathbf{U}_{tan}$ the tangential component of $\mathbf{U}$ and $c > 0$. We write the derivatives of $\mathbf{U}$ in the special edge parameterization (w_1, w_2) as the follows.

$$\frac{\partial \mathbf{U}}{\partial w_i} = a_i\mathbf{U} - c_{n,i}\mathbf{n} - b_i\mathbf{y}_1 \tag{10}$$

where $i = 1, 2$ and $\mathbf{n}$ is the normal to the medial sheet at $\mathbf{x}_0$. Then in matrix form the edge shape operator is

$$\mathbf{S}_E = \begin{pmatrix} b_1 & b_2 \\ c_{n,1} & c_{n,2} \end{pmatrix} \tag{11}$$

Let $I_{1,1} = \begin{pmatrix} 1 & 0 \\ 0 & 0 \end{pmatrix}$. The generalized eigenvalue of $(\mathbf{S}_E, I_{1,1})$ is defined to be the *principal edge curvature* κ_E. The legality of the crest boundary implied by the end spokes is guaranteed if $\kappa_E < 1$ for the positive principal edge curvature κ_E.

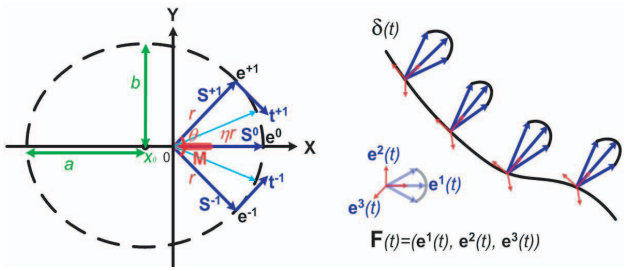

Figure 3. Left: three spokes $\mathbf{S}^{+1/-1/0}$ (thick arrows in dark blue) with length $r/r/\eta n$ of an end atom forming a plane; interpolated spokes (thin arrows in cyan) filling the gaps between the three spokes of each end atom; the medial sheet of the partial ellipse fit to the three spoke ends is $\mathbf{M}$, the thick red segment on $\mathbf{S}^0$ bisector spoke. Right: planar curves sweeping along the end curve $\delta(t)$ of the medial sheet; a local frame implied by end atom spokes also sweeps along $\delta(t)$, forming a frame field $\mathbf{F}(t)$.

This condition can be easily checked given the crest region generation from sweeping planar curves. To avoid jumping into the simple form of the edge curvature condition without understanding the prerequisite, next we will describe how each planar curve is created from each interpolated end atom and introduce the setup for the curve sweeping. Then we will revisit the crest legality condition in its simple form based on the generated crest.

3.3.2 Interpolating planar curves

Based on the fact that the three spokes of each end atom stay in the same plane (fig. 3), we fit a curve as a part of an ellipse, the medial sheet of which is a segment on the bisector spoke $\mathbf{S}^0$, to pass through the ends of the three spokes. Furthermore the ellipse curve is perpendicular to the spokes $\mathbf{S}^{+1/-1/0}$ at all the corresponding spoke ends, providing G^1 continuity from the internal atom implied boundary to the crest region swept by the series of such planar curves.

The three planar spokes of an end atom are shown in fig. 3 left. Without loss of generality, the spokes and the ellipse fitting are described in $\mathbb{R}^2$. The result of the fitting can be applied to the actual spokes in 3D by a direct change of coordinates.

With the ellipse given by $\frac{(x-x_0)^2}{a^2} + \frac{y^2}{b^2} = 1$, the constraints are as follows: spoke ends $\mathbf{e}^{+1/-1} = (x_L, \pm y_L), \mathbf{e}^0 = (x_R, 0)$, and the tangential directions at ends of $\mathbf{e}^{+1/-1}$ as $\mathbf{t}^{+1/-1} = (y_L, \mp x_L)$. Due to the symmetry of $\mathbf{e}^{+1/-1}$ and $\mathbf{t}^{+1/-1}$, there are three real constraints with three unknown parameters for the ellipse. (a, b, x_0) can be uniquely solved

as follows,

$$x_0 = \frac{x_L(x_L^2 - x_R^2 + y_L^2)}{2x_L^2 - 2x_L x_R + y_L^2} \quad (12)$$

$$a = \frac{-x_L^3 + x_R(2x_L^2 + y_L^2) - x_L(x_R^2 + y_L^2)}{2x_L^2 - 2x_L x_R + y_L^2} \quad (13)$$

$$b = \sqrt{\frac{(x_L^2 - x_L x_R + y_L^2)^2}{2x_L^2 - 2x_L x_R - y_L^2}} \quad (14)$$

as long as $2x_L^2 - 2x_L x_R - y_L^2 > 0$ and $-x_L^2 + x_R(2x_L + y_L^2) - x_L(x_R^2 + y_L^2) > 0$. Let $(x_L, y_L) = (r\cos(\theta), r\sin(\theta)), x_R = \eta r$, where r is the regular spoke length, θ is the angle between two regular spokes $\mathbf{S}^{+1/-1}$, $\mathbf{e}^{+1/-1}$ in this case, and η is the bisector length factor (fig. 3 left). The two conditions above might be violated only when θ and η have extreme values. In practice, we maintain $\theta \in (\frac{\pi}{3}, \frac{2\pi}{3})$ and $\eta \in (1.05, 1.2)$ in reasonable ranges; with these ranges (a, b, x_0) have been successfully solved for synthetic and real world objects.

Moreover, the medial sheet of the part of ellipse is the segment lying on the bisector spoke, shown in fig. 3 left as the thick red segment **M**. Given that, interpolated spokes, shown as the cyan spokes in fig. 3 left, are analytically calculated and filled in the two gaps between the three spokes.

The partial ellipse curve then sweeps along while the end atom travels along the end curve $\delta(t)$, generating a swept surface for the entire crest region, shown in fig. 3 right. Each end atom also determines a local frame $\mathbf{F}(\mathbf{e}_1, \mathbf{e}_2, \mathbf{e}_3)$ shown in fig. 3 right, which sweeps along the end curve $\delta(t)$ as well and forms a frame field $\mathbf{F}(t) = (\mathbf{e}_1(t), \mathbf{e}_2(t), \mathbf{e}_3(t))$ on $\delta(t)$. All these are necessary for the legality condition of the crest, described next.

3.3.3 Simple legality condition for the crest

Given the local frame field $\mathbf{F}(t)$ on the end curve $\delta(t)$ parameterized by t, the derivative of $\delta(t)$ can be written in $\mathbf{F}(t)$.

$$\delta' = r_1\mathbf{e}_1 + r_2\mathbf{e}_2 + r_3\mathbf{e}_3 \quad (15)$$

In $\mathbf{F}(t), \mathbf{e}_1(t)$ is the unit bisector spoke direction U^0, so

$$\mathbf{U}' = \mathbf{e}_1' = \omega_{12}\mathbf{e}_2 + \omega_{13}\mathbf{e}_3 \quad (16)$$

By Damon, the principal edge curvature κ_E falls out as the following simple form.

$$\kappa_E = -\frac{\omega_{13}}{r_3} \quad (17)$$

This κ_E is used in the edge curvature condition $r\kappa_E < 1$ for the crest region, where r is the spoke length. This condition is checked on samples, i.e. the interpolated end atoms and their corresponding planar curves. If the legality condition failed to hold at any of the sample, we would resolve it by changing the η interpolation, although we have not seen such a failed case in the testing objects.

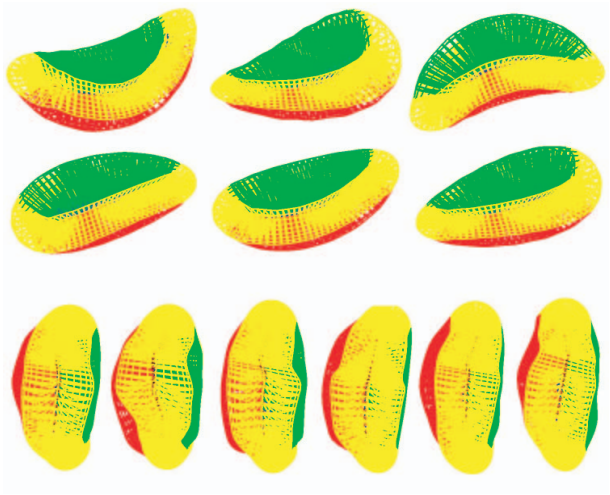

Figure 4. Top: interpolation results on synthetic ellipsoid m-reps. Bottom: interpolation results on real-patient kidney m-reps.

We applied the internal and end atom interpolation to some synthetic and real-world m-reps. The results are shown in the next section.

4. Results and Discussion

The application of our interpolation method on a given single figure m-rep yields a continuous double-sided spoke field on a smooth medial sheet. We used both synthetic ellipsoids and real-patient kidneys as the test objects..

4.1. Results

The synthetic ellipsoids are generated by applying three statistically independent global deformations to the local discrete atoms, namely bending, twisting, and tapering. Each basic deformation is controlled by a variable sampled from a uniform distribution and applied on an m-rep created from a standard ellipsoid. We also have 39 kidney m-reps segmented from real-patient images as the real-world test objects. The interpolation results are shown in fig. 4: the red and green boundary meshes are implied by the interpolated regular spokes on both sides of the medial sheet; the yellow sweeping planar curves from the end atom interpolation form the crest region.

4.2. Open issues and potential solutions

As an on-going research project, there are some open issues on our interpolation method. We describe these issues, show the potential solutions, then conclude this paper.

The internal atom interpolation using $r\mathbf{S}_{rad}$ is currently implemented for single figure m-reps. Here are three remaining issues and the corresponding possible solutions:

1. Speed: each interpolation is calculated by a local integration of the radial shape operators. The improvement lies in the analytical integration instead of the current numerical solution.

2. Continuity: C^2 or G^2 continuity is sufficient for most applications. Currently C^0 continuity is enforced across interpolated patches. Recall that the $r\mathbf{S}_{rad}$'s at the control atoms are initially estimated by finite differences. The plan to improve the continuity is to optimize on the initial $r\mathbf{S}_{rad}$'s until the integration of the interpolated spokes converge to the spokes at the control atoms.

3. Umbilic points: in section 3.2.4 we showed the potential problem with the current $r\mathbf{S}_{rad}$ interpolation. The $r\mathbf{S}_{rad}$ matrix does not have a real eigen-decomposition at a medial umbilic point. One possible solution for this is to interpolate $\lambda\mathbf{I} - r\mathbf{S}_{rad}$ instead of $r\mathbf{S}_{rad}$, with constant $\lambda > 1$, in the $GL^+(2)$ group, and convert the interpolated matrix back to $r\mathbf{S}_{rad}$. Because of the legality condition, we can pick $\lambda > 1$ as a constant. Then $\mathbf{S}^{'} = \lambda I - r\mathbf{S}_{rad}$ is positive definite, i.e., $\mathbf{S}^{'} \in GL^+(2)$. An interpolation of $\mathbf{S}^{'}$ in the $GL^+(2)$ group can solve the problem of having any umbilic points.

Given the quad-mesh in discrete m-reps, the end curve is only C^0 at the four "corners". We plan to improve this by slightly changing the medial sheet $\mathbf{x}(v_1, v_2)$ interpolation to remove the corners.

In this paper we have proposed an interpolation method in discrete m-reps. Internal atoms of an m-rep are interpolated by the integration via interpolated $r\mathbf{S}_{rad}$'s on the smooth medial sheet, and end atoms are interpolated by partial ellipses fit to end atom spoke ends and the crest is a swept surface by the planar ellipse curves along the end medial curve. We maintain the legality of the interpolated internal atoms and detect any illegality in the crest regions. Results show our method applies well to both synthetic and real-world objects.

The ability of deriving a continuous representation from a discrete m-rep by interpolation opens more doors for discrete m-reps by having a continuous object representation while still having the localized control via the discrete medial atoms. Also, since discrete m-reps provide the useful capability of representing objects with multiple parts, we are currently extending the interpolation to the blends between the parts.

5. Acknowledgement

We'd like to thank all the people in the MIDAG group for helpful discussions, and P. Thomas Fletcher for the suggestion on the medial umbilic points. The work reported here was done under the partial support of NIH grant P01 EB02779.

References

[1] P. T. Fletcher, C. Lu, S. M. Pizer, and S. Joshi. Principal geodesic analysis for the nonlinear study of shape. *Transactions on Medical Imaging*, 23(8):995–1005, 2004. 1, 2

[2] R. Broadhurst, J. Stough, S. Pizer, and E. Chaney. A statistical appearance model based on intensity quantiles. *To appear*. International Symposium on Biomedical Imaging (ISBI), 2006. 1

[3] P. Yushkevich, P. T. Fletcher, S. Joshi, A. Thall, and S. M. Pizer. Continuous medial representations for geometric object modeling in 2d and 3d. *Image and Vision Computing*, 21(1):17–28, 2003. 1

[4] P. A. Yushkevich, H. Zhang, and J. C. Gee. Parametric medial shape representation in 3-d via the poisson partial differential equation with non-linear boundary conditions. In G. E. Christensen and M. Sonka, editors, *IPMI2005, LNCS 3565*, pages 162–173. IPMI, Springer-Verlag, 2005. 1

[5] S. M. Pizer, T. Fletcher, Y. Fridman, D. S. Fritsch, A. G. Gash, J. M. Glotzer, S. Joshi, A. Thall, G. Tracton, P. Yushkevich, and E. L. Chaney. Deformable m-reps for 3d medical image segmentation. *International Journal of Computer Vision - Special UNC-MIDAG issue*, 55(2):85–106, 2003. 1

[6] S. M. Pizer, T. P. Fletcher, S. Joshi, G. A. Gash, J. Stough, A. Thall, G. Tracton, and E. L. Chaney. A method and software for segmentation of anatomic object ensembles by deformable m-reps. *American Association of Physicists in Medicine*, 32(5):1335–1345, May 2005. 1

[7] J. N. Damon. Smoothness and geometry of boundaries associated to skeletal structures i: Sufficient conditions for smoothness. *Annales de Institut Fourier*, 53(6):1941–1985, 2003. 2

[8] J. N. Damon. Smoothness and geometry of boundaries associated to skeletal structures ii: Geometry in the blum case. *Compositio Mathematica*, 2003. 2

[9] J. N. Damon. Determining the geometry of boundaries of objects from medial data. *International Journal of Computer Vision*, 61(1):45–64, 2005. 2

[10] Q. Han, C. Lu, S. Liu, S. M. Pizer, S. Joshi, and A. Thall. Representing multi-figure anatomical objects. In *IEEE International Symposium on Biomedical Imaging (ISBI)*, pages 1251–1254. ISBI, 2004. 2

[11] Q. Han, S. M. Pizer, D. Merck, S. Joshi, and J.-Y. Jeong. Multi-figure anatomical objects for shape statistics. In G. E. Christensen and M. Sonka, editors, *IPMI2005, LNCS 3565*, pages 701–712. IPMI, Springer-Verlag, 2005. 2

[12] A. Thall. Deformable solid modeling via medial sampling and displacement subdivision. *PdD thesis, Dept. of Comp. Sci., UNC @ Chapel Hill*, 2004. 2

[13] H. Blum and R. Nagel. Shape description using weighted symmetric axis features. *Pattern Recognition*, 10:167–180, 1978. 3